UV-resonance Raman spectroscopy of amino acids

Martin Höhl, Merve Meinhardt-Wollweber, Heike Schmitt, Thomas Lenarz, Uwe Morgner

Martin Höhl, Merve Meinhardt-Wollweber, Heike Schmitt, Thomas Lenarz, Uwe Morgner, "UV-resonance Raman spectroscopy of amino acids," Proc. SPIE 9704, Biomedical Vibrational Spectroscopy 2016: Advances in Research and Industry, 970404 (7 March 2016); doi: 10.1117/12.2212781

SPIE.

Event: SPIE BiOS, 2016, San Francisco, California, United States

UV-Resonance Raman Spectroscopy of Amino Acids

Martin Höhl[*a,c], Merve Meinhardt-Wollweber[a,c], Heike Schmitt[b,c], Thomas Lenarz[b,c], Uwe Morgner[a,c]

[a]Institut für Quantenoptik, Leibniz Universität Hannover, Welfengarten 1, 30167 Hannover, Germany; [b]Experimentelle Otorhinolaryngologie, Medizinische Hochschule Hannover, Carl-Neuberg-Straße 1, 30625 Hannover, Germany; [c]Cluster of Excellence "Hearing4all"

ABSTRACT

Resonant enhancement of Raman signals is a useful method to increase sensitivity in samples with low concentration such as biological tissue. The investigation of resonance profiles shows the optimal excitation wavelength and yields valuable information about the molecules themselves. However careful characterization and calibration of all experimental parameters affecting quantum yield is required in order to achieve comparability of the single spectra recorded. We present an experimental technique for measuring the resonance profiles of different amino acids. The absorption lines of these molecules are located in the ultraviolet (UV) wavelength range. One limitation for broadband measurement of resonance profiles is the limited availability of Raman filters in certain regions of the UV for blocking the Rayleigh scattered light. Here, a wavelength range from 244.8 nm to 266.0 nm was chosen. The profiles reveal the optimal wavelength for recording the Raman spectra of amino acids in aqueous solutions in this range. This study provides the basis for measurements on more complex molecules such as proteins in the human perilymph. The composition of this liquid in the inner ear is essential for hearing and cannot be analyzed non-invasively so far. The long term aim is to implement this technique as a fiber based endoscope for non-invasive measurements during surgeries (e. g. cochlear implants) making it available as a diagnostic tool for physicians. This project is embedded in the interdisciplinary cluster of excellence "Hearing for all" (H4A).

Keywords: Raman, resonance, uv, amino acid, perilymph

1. INTRODUCTION

Raman spectroscopy can be used to gather a wealth of information about a molecule non-destructively [1-4]. For measuring molecules at small concentrations or investigating many different properties of a molecule at the same time, a high sensitivity is needed. Resonance Raman Spectroscopy (RRS) enables a much higher signal-to-noise-ratio (SNR) without requiring major changes to the experimental setup compared to normal Raman scattering. The excitation of Raman scattered light near an absorption line of a molecule leads to an increase in the generated signal of several orders of magnitude [5,6]. In case of amino acids, the absorption of light mainly takes place in the deep UV. Examples of amino acid absorption spectra are shown in Figure 1. To demonstrate the resonant enhancement in the UV, we investigated proline and glycine making use of their good solubility in water. The solvent itself shows no remarkable Raman signatures in the so-called fingerprint region (500 rel. cm^{-1} to 1700 rel. cm^{-1}). Optimal resonance enhancement is usually achieved by choosing an excitation wavelength in the main absorption range. However, also pre-resonant conditions may lead to considerable signal gain and might, thus, be advantageous for some molecules.

Here, we present an experimental technique on how to acquire the UV Raman spectra and a method for data post-processing. The latter is essential to make the single spectra comparable to each other in terms of relative wavenumbers and Raman line intensities. Combining all spectra in one graph leads to a so-called Excitation-Emission-Map (EEM) as further detailed in Figure 3. Raman peaks appear as (vertical) lines that are characteristic for each molecule. The intensity of these lines reveals the optimal wavelength for recording the Raman spectrum of the corresponding molecule and grants information about that molecule [7-9].

[*] martin.hoehl@hot.uni-hannover.de; phone 49 511 762-17924; fax 49 511 762-17909; hearing4all.eu

Biomedical Vibrational Spectroscopy 2016: Advances in Research and Industry, edited by Anita Mahadevan-Jansen, Wolfgang Petrich, Proc. of SPIE Vol. 9704, 970404
 · doi: 10.1117/12.2212781

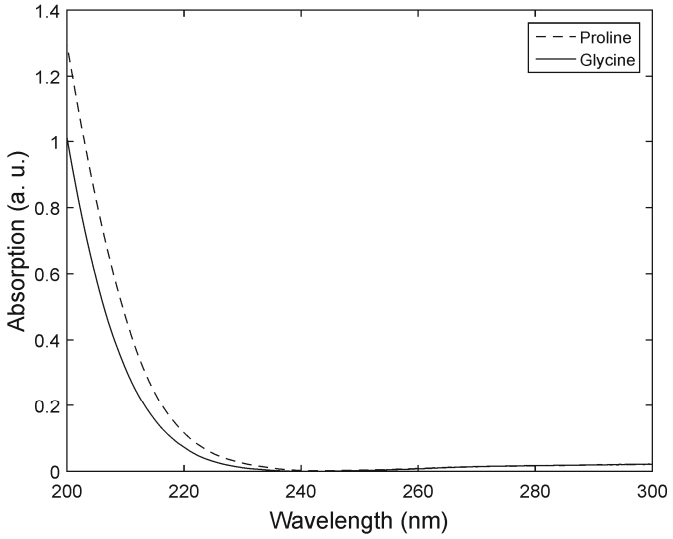

Figure 1. Absorption spectra of proline and glycine acquired using a spectrophotometer (Kontron Instruments Uvikon 931). Concentrations were chosen to properly fit the measurement range of the spectrophotometer.

2. EXPERIMENTAL SETUP

The experimental setup for measuring the resonance enhancement for amino acids is shown in Figure 2. The light source utilized is an Optical Parametric Oscillator (OPO, Ekspla PG122/UV) that delivers nanosecond pulses in the UV. A small part of the pulse energy is picked by a beamsplitter (B, fused silica) and reflected onto a photodiode (PD, Thorlabs DET10A/M). The diode was calibrated with a pulse energy meter (Thorlabs ES111C) to monitor the energy of the individual excitation pulses. The main part of the light is focused (L1) inside a cuvette (C, fused silica, 10 mm light path) containing the amino acids in solution. The Raman scattered light is collected via a second lens (L2) and sent through a long-pass filter (LP, Semrock SEM-LP02-248RS-25, SEM-LP02-257RU-25, or SEM-LP02-266RU-25, respectively) for blocking the Rayleigh-scattered light. The signal generated this way is focused into a fiber (F, Thorlabs UM22-100) that guides the light to a spectrometer (Andor Shamrock SR-500i-C-R with Andor Newton DU940P-BU) for detection.

The spectra measured with this setup require post-processing in order to make them comparable to each other. The extinction of excitation and Raman-shifted light through the optical system is wavelength dependent and so is the detection efficiency of the camera attached to the spectrometer. To take these effects into account for the intensity and wavenumber correction of the Raman signals, the Device Spectral Response Function (DSRF) was determined. For each wavelength that needs to be considered for setting up an EEM, one single pulse was emitted by the OPO, sent through the (whole) experimental setup and was finally recorded by the spectrometer. The spectrum was then fitted by a Voigt-profile to obtain the peak height as a figure-of-merit (FoM). This procedure is repeated five times to determine the average DSRF. This function is used in all subsequent measurements to adjust the recorded spectra.

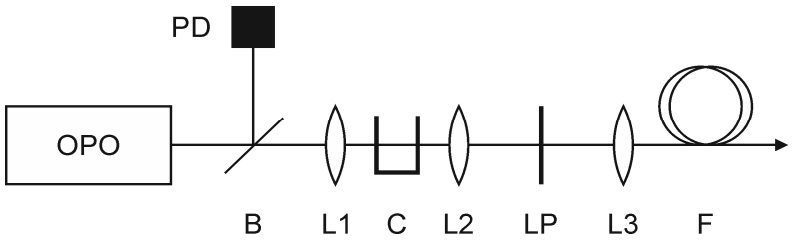

Figure 2. Experimental setup for investigating the resonance enhancement of amino acids (OPO: Optical Parametric Oscillator, B: Beamsplitter, PD: Photodiode, L1: f = 20 mm lens, C: Cuvette, L2: f = 20 mm lens, LP: Long-pass filter, L3: f = 50 mm lens, F: Fiber).

3. RESULTS

The light source used in the experimental setup emits nanosecond laser pulses tunable in the range from 210.0 nm to 354.0 nm. Since there is only limited availability of Raman-filters, a range from 244.8 nm to 266.0 nm was selected to demonstrate the resonant enhancement. The chosen constellation of three long-pass filters leads to an EEM that is subdivided into three areas, one for each filter (see Figures 3b and d). The first region ranges from 244.8 nm to 249.7 nm, the second from 252.4 nm to 257.6 nm, and the third from 260.3 nm to 266.0 nm. The short wavelength limits were chosen to allow at least half of the fingerprint region (500 rel. cm^{-1} to 1700 rel. cm^{-1}) to pass the long-pass filters. The long wavelength limits are determined by the highest wavelengths that are still sufficiently attenuated by these filters.

For measuring the EEMs shown in Figures 3b and d, the amino acids proline and glycine were solved in water. Both show a high solubility leading to high concentrations in the solvent and, thus, short exposure times. The energy output of the OPO is wavelength dependent. As a compromise between high SNR and short exposure time, the irradiated amount of energy was set to 250 mJ for each spectrum. The calibrated photodiode tracked the actually applied energies in the samples.

After recording of Raman spectra with many different wavelengths, post-processing of the raw data is required. The spectra in Figure 3 were obtained after several steps of processing. First, artifacts originating from cosmic rays were removed. The vicinity to the absorption lines of the molecules may lead to a fluorescence background that was also subtracted for each spectrum. In the next step, the DSRF was applied. Every intensity value of an EEM was divided by a correction factor to account for the spectral behavior of the experimental setup. Finally, the non-molecule specific wavelength dependence of Rayleigh/Raman-scattering cross sections (λ^{-4}) and the actual energy applied were compensated. The former is done by multiplying with the ratio of the current and the smallest wavelength to the power of four and the latter is accounted for by dividing with the energy measured via the photodiode.

The shape of vertical intensity lines in an EEM reflects the resonance enhancement of a specific Raman feature. Both maps presented in Figure 3 show a resonance behavior for the most significant Raman peaks which are characteristic for these molecules. For proline, the strongest Raman line is located at 1395 rel. cm^{-1} and for glycine the two strongest lines are found at 1318 rel. cm^{-1} and 1400 rel. cm^{-1}, respectively. These positions were determined by fitting the spectra with a Voigt-profile at the estimated locations. As can be seen in Figures 3b and d, the Raman intensity of these lines is considerably increased when excited at shorter wavelengths even though excitation conditions are only pre-resonant.

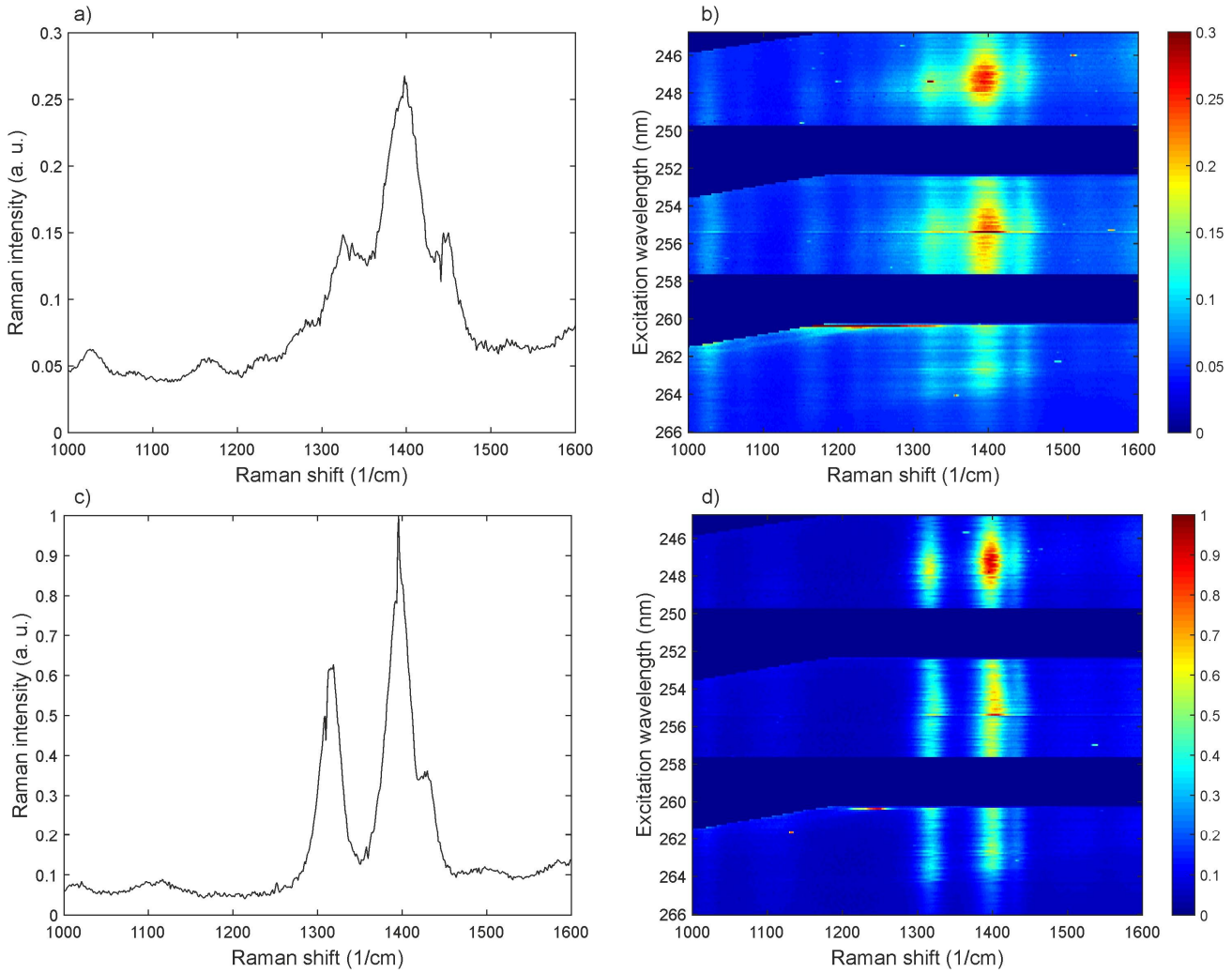

Figure 3. Resonance Raman spectra of proline (a, b) and glycine (c, d). The spectra on the left side correspond to the rows with the highest Raman signal from the EEMs on the right side (for proline: $\lambda = 247.0$ nm, for glycine: $\lambda = 247.8$ nm).

4. CONCLUSION

The experimental setup presented here is able to measure the Raman spectra of amino acids in the ultraviolet wavelength range. The data post-processing approach allows investigating the resonance enhancement of molecules over a broad range of wavelengths. Going even deeper into the UV would lead to a stronger resonance enhancement. However, in this case, background fluorescence may increase requiring a suitable mechanism for background reduction.

The spectral information obtained in this work will be used for subsequent measurements on more complex molecules such as proteins. Their absorption is shifted to longer wavelengths but still lies in the UV. Our long term goal is to develop a technique to analyze native samples of human perilymph. This would then allow to gain access to pathophysiological parameters such as the protein content of the inner ear liquid which is of relevance for medical diagnosis of hearing impairment at an early stage. For this purpose, we plan to realize a fiber based endoscope suitable for Raman measurements during surgical interventions.

ACKNOWLEDGMENT

We would like to thank the DFG (Deutsche Forschungsgemeinschaft) for funding within the cluster of excellence "Hearing4all".

REFERENCES

[1] Oladepo, S. A., Xiong, K., Hong, Z. and Asher, S. A., "Elucidating Peptide and Protein Structure and Dynamics: UV Resonance Raman Spectroscopy," J. Phys. Chem. Lett., 2(4), 334-344 (2011).

[2] Podstawka-Proniewicz, E., Piergies, N., Skołuba, D., Kaferski, P., Kim, Y. and Proniewicz, L. M., "Vibrational Characterization of l-Leucine Phosphonate Analogues: FT-IR, FT-Raman, and SERS Spectroscopy Studies and DFT Calculations," J. Phys. Chem. A, 115(40), 11067-11078 (2011).

[3] Vass, E., Hollósi, M., Besson, F. and Buchet, R., "Vibrational Spectroscopic Detection of Beta- and Gamma-Turns in Synthtic and Natural Peptides and Proteins," Chem. Rev., 103(5), 1917-1954 (2003).

[4] Kniggendorf, A.-K., Meinhardt-Wollweber, M., Yuan, X., Roth, B., Seifert, A., Fertig, N. and Zeilinger, C., "Temperature-sensitive gating of hCx26: high-resolution Raman spectroscopy sheds light on conformational changes," Biomed. Opt. Express, 5(7), 2054-2065 (2014).

[5] Asher, S. A., "UV Resonance Raman Spectroscopy for Analytical, Physical, and Biophysical Chemistry Part 1," Anal. Chem., 65(2), 59A-66A (1993).

[6] Asher, S. A., "UV Resonance Raman Spectroscopy for Analytical, Physical, and Biophysical Chemistry Part 2," Anal. Chem., 65(4), 201A-210A (1993).

[7] Chi, Z., Chen, X. G., Holtz, J. S. W. and Asher, S. A., "UV Resonance Raman-Selective Amide Vibrational Enhancement: Quantitative Methodology for Determining Protein Secondary Structure," Biochemistry, 37(9), 2854-2864 (1998).

[8] Zhao, X. and Spiro, T. G., "Ultraviolet Resonance Raman Spectroscopy of Hemoglobin with 200 and 212 nm Excitation: H-Bonds of Tyrosines and Prolines," J. Raman Spectrosc., 29(1), 49-55 (1998).

[9] Rwere, F., Mak, P. J. and Kincaid, J. R., "Resonance Raman determination of vinyl group disposition in different derivatives of native myoglobin and its heme-disoriented form," J. Raman Spectrosc., 45(1), 97-104 (2014).